The Journal of Immunology

TLR9 Activation Coupled to IL-10 Deficiency Induces Adverse Pregnancy Outcomes

Jessica E. Thaxton, Roberto Romero and Surendra Sharma

References	This article **cites 60 articles**, 14 of which you can access for free at: http://www.jimmunol.org/content/183/2/1144.full#ref-list-1

Why *The JI*? Submit online.

- **Rapid Reviews! 30 days*** from submission to initial decision

- **No Triage!** Every submission reviewed by practicing scientists

- **Fast Publication!** 4 weeks from acceptance to publication

*average

Subscription	Information about subscribing to *The Journal of Immunology* is online at: http://jimmunol.org/subscription
Permissions	Submit copyright permission requests at: http://www.aai.org/About/Publications/JI/copyright.html
Email Alerts	Receive free email-alerts when new articles cite this article. Sign up at: http://jimmunol.org/alerts

TLR9 Activation Coupled to IL-10 Deficiency Induces Adverse Pregnancy Outcomes[1]

Jessica E. Thaxton,* Roberto Romero,[†] and Surendra Sharma[2]*

Pregnancy outcome is severely compromised by intrauterine infections and inflammation. Although the pregnant uterine micro-environment is replete with innate immune cells and TLR expression, the mechanisms that facilitate adverse effects of their activation are largely unknown. In this study, we mimic the activation of TLR9 with its pathogenic ligand hypomethylated CpG and demonstrate that IL-10 proficiency protects against CpG-induced pregnancy complications. We show that fetal resorption and preterm birth are rapidly induced in IL-10$^{-/-}$ mice by low doses of CpG (~25 μg/mouse) when injected i.p. on gestational day 6 or gestational day 14, respectively. In contrast, wild-type mice failed to experience such effects at comparable doses, but pups born at term displayed craniofacial/limb defects in response to higher doses (~400 μg/mouse). Pregnancy complications in IL-10$^{-/-}$ mice were associated with unexpected and robust TLR9-triggered activation and amplification of uterine neutrophil and macrophage subpopulations followed by their migration to the placental zone. Furthermore, a dramatic increase in serum levels of mouse KC and TNF-α production by uterine F4/80$^+$ cells, but not uterine NK or Gr-1$^+$CD11b$^+$ cells, was observed. Depletion of F4/80$^+$ macrophages or neutralization of TNF-α rescued pregnancy to term. Our results have important implications for IL-10-mediated "uterine tolerance" against CpG-driven innate immune activation. *The Journal of Immunology,* 2009, 183: 1144–1154.

A common link for a significant proportion of early and late pregnancy maladies lies in intrauterine infections and inflammation (1, 2). In this regard, the role of the innate immune system at the maternal-fetal interface in response to normal pregnancy intrauterine milieu or inflammatory stimuli has attracted an abundance of recent interest. Although a vigorous uterine immune system juxtaposes the fetal tissue predominated by innate sentinels, NK cells and macrophages, it does not pose any intolerance to normal fetal development and survival of invading trophoblasts (3–5). We and others have proposed that uterine NK (uNK)[3] cells produce angiogenic and pregnancy-compatible factors and are involved in local endovascular processes and regulation of trophoblast invasion (3, 6–8). On the other hand, in a mouse model, we have demonstrated that uNK cells become antagonistic to pregnancy in response to bacterial products (9, 10). Thus, the underlying mechanisms of diverse pathogen-mediated inflammatory events that may trigger cytotoxic activation of maternal immune cells and trophoblasts require further exploration.

A group of innate immune sentinel receptors known as TLRs are present not only on uterine leukocytes, but also on trophoblast cells, thus implying an active cross-talk between the placenta and local immunity (11–13). TLRs have evolved to recognize specific pathogen-associated molecular patterns enabling them to serve as the first line of defense in the innate immune system (14, 15). Although TLRs are ancient receptors without memory requirements for cells that express them, they harbor the ability to transduce both negative and positive signals depending on interactions with their immediate microenvironment (16). Moreover, pathogenic load and gene-environment interactions are likely to be overriding factors in the outcome of inflammation-induced positive versus negative cascades. Our recent studies provide support to this hypothesis in that very low doses of LPS cause adverse pregnancy outcomes in IL-10$^{-/-}$ mice compared with their wild-type (WT) counterparts (9, 10).

Systemic or intrauterine bacterial and viral infectious agents, and their breakdown products, are likely to lead to the excessive presence of pathogenic hypomethylated CpG DNA motifs which are recognized by TLR9 (17, 18). Few studies have focused on the role of TLR9-mediated immune activation during pregnancy. Using C57BL/6 mice, it has been shown that high doses of CpG cause deformities in pups born to treated dams (19). On the other hand, CpG has been used as an adjuvant to reduce negative fetal outcomes induced by *Listeria monocytogenes* in BALB/c pregnant dams (20). In other settings, it has been shown that direct injection of CpG DNA in neuroblastomas induces complete tumor rejection in mice and elicits long-term Th1-driven immunity (21). In addition, antitumor effects of CpG have been demonstrated in different intracranial models of syngeneic glioma (22, 23). These observations imply that CpG motifs are capable of triggering strong and polarized immune responses which may be beneficial or harmful depending on the intrinsic microenvironment.

*Department of Pediatrics, Women and Infants Hospital of Rhode Island, Warren Alpert Medical School of Brown University, Providence, RI 02905; and [†]Perinatology Research Branch, Eunice Kennedy Shriver National Institute of Child Health and Human Development, National Institutes of Health/Department of Health and Human Services, Detroit, MI 48201

[2] Address correspondence and reprint requests to Dr. Surendra Sharma, Department of Pediatrics, Women and Infants Hospital, 101 Dudley Street, Providence, RI 02905. E-mail address: ssharma@wihri.org

[3] Abbreviations used in this paper: uNK, uterine NK; ODN, oligodeoxynucleotide; UMGC, uterine mononuclear and granular cells; DHR, dihydrorhodamine 123; gd, gestational day; ROS, reactive oxygen species; mKC, mouse KC.

Given the proposed widespread use of CpG as a treatment and vaccine tool among the general population, including pregnant individuals, it is important to determine whether overactivation of the immune system in response to nonteratogenic doses of CpG can lead to negative pregnancy outcomes (20, 24–28). In this study, we examined the role of the CpG-TLR9 axis in a mouse model of pregnancy with a focus on the protective role of pregnancy-compatible cytokines such as IL-10. CpG-induced TLR9 activation has been associated mainly with stimulation of systemic immunity. Our observations allow us to elucidate a link between CpG-mediated activation of innate immune responses and IL-10 deficiency at the maternal-fetal interface that leads to adverse pregnancy outcomes.

Materials and Methods

Mice

Mice used in this study, C57BL/6 and C57BL/6 IL-10$^{-/-}$, were obtained from The Jackson Laboratory. All mice were housed in a specific pathogen-free facility supervised by the Central Research Department of Rhode Island Hospital. All protocols were approved by the Lifespan Animal Welfare Committee and conducted according to its guidelines. Mice of 8–10 wks of age were mated and each experimental group contained at least three mice. The day of vaginal plug appearance was designated gestational day (gd) 0.

In vivo treatment of pregnant mice

WT and IL-10$^{-/-}$ mice received i.p. injections of CpG oligodeoxynucleotide (ODN 1826; InvivoGen) at doses of 15, 25, 100, 300, or 400 μg on gd6 or gd14. For IL-10$^{-/-}$ mice, suitable doses were 15 or 25 μg/dam since higher doses caused maternal demise. Cellular depletions were performed with CpG injection on gd6 or gd14. One hundred microliters of anti-asialo GM1 (Wako) or nonimmune rabbit serum (Antibodies) was administered on gd4, 6, and 9 or gd9, 11, and 14 for NK cell depletion. Two hundred fifty micrograms of anti-Gr-1 (RB6-8C5; BD Biosciences) or isotype Ab (rat IgG1; BD Biosciences) was administered at gd5. Two hundred fifty micrograms of anti-F4/80 (BM8; eBioscience) or isotype Ab (rat IgG2a, κ; eBioscience) was given on gd5 and 7 or gd13 and 15. Competitive antagonist experiments were performed in IL-10$^{-/-}$ mice and i.p. injections of 100 μg or 50 μg of antagonist ODN (ODN 2088; InvivoGen) were given with 25 μg of CpG ODN on gd6. Control experiments were performed using 50 or 100 μg of antagonist ODN alone or 50 or 100 μg of antagonist ODN plus 25 μg of CpG ODN on gd6. Monoclonal anti-TNF-α Ab (Gr81-2626; BD Pharmingen) was administered i.p. at 250 μg on gd5 and gd7 with CpG ODN injection on gd6 or on gd13 and gd15 with CpG ODN injection on gd14.

Cellular preparation

Uterine mononuclear and granular cells (UMGC) were obtained via mincing and mechanical dispersion of whole gd 8–9 or gd15 uteroplacental tissue in RPMI 1640 supplemented with 10% FBS, penicillin/streptomycin, and L-glutamine. Single-cell suspensions from uterine horns were run through a 100-μm cell strainer and subjected to density gradient separation using Fico-Lite LM (Atlanta Biologicals). Experiments were performed on the three layers obtained from Ficoll gradient separation to determine in which layer granulocytes accumulated. It was found that granulocytes collect directly below the monocyte layer and both layers were harvested together for all experiments.

Flow cytometry

Abs to NK1.1 (NKR-PIC), CD3 (145-2C11), CD45 (30-F11), F4/80 (BM8), Gr-1(RB6-8C5), CD11b (M1/79), and Ly6G (1A8) were purchased (BD Biosciences). Isolated UMGC were washed in PBS and resuspended in PBS containing 2% FBS (stain buffer). Combinations of Abs were added for extracellular staining for 30 min at 4°C, rinsed with stain buffer, and acquired via flow cytometry (FACSCanto; BD Biosciences). Fluorochrome-conjugated isotype-matched Abs were used as controls. Abs to TNF-α (MP6-XT22) and IFN-γ (XMG1.2) were purchased for intracellular staining (BD Biosciences). UMGC were washed with stain buffer and incubated in 96-well plates for 4–6 h with Brefeldin A (BD Biosciences), PMA (Calbiochem), and ionomycin (Calbiochem). Cells were washed twice with stain buffer and stained extracellularly as described above. For intracellular staining, UMGC were washed with Perm Wash (BD Biosciences) and fixed with Cytofix/Cytoperm (BD Biosciences) for 25 min at

4°C and incubated with Abs for 30 min at room temperature. Cells were washed and analyzed via flow cytometry.

Intracellular reactive oxygen species (ROS) production was assessed with dihydrorhodamine 123 (DHR; Sigma-Aldrich) by flow cytometry. This nonfluorescent dye becomes fluorescent upon oxidation to rhodamine by ROS produced during the respiratory burst. Directly after UMGC were prepared, DHR (10 μmol/ml) was added simultaneously with Abs Gr-1, CD45, and CD11b or with irrelevant isotype Abs, and the mixture was incubated at 37°C for 15 min. UMGC were washed and immediately processed by flow cytometry.

ELISA

TNF-α, IL-12, IFN-γ, mouse KC (mKC), MIP-1α, and MIP-2 were measured in serum. Blood samples were collected via cardiac puncture into 1-ml tubes, allowed to clot for 30 min at room temperature, spun at 8000 rpm for 20 min at 4°C, and supernatants were collected and frozen for further analysis. TNF-α, IL-12, IFN-γ, mKC, MIP-1α, and MIP-2 were assayed using Quantikine ELISA kits (R&D Systems) and experiments were performed according to the manufacturer's instructions. Separate serum samples were collected from each experimental treatment group (n = 9).

Immunohistochemistry

Fetoplacental units from varying experimental conditions were removed from uterine horns and placed in 4% buffered formalin or snap frozen in a cassette with OCT. Samples in the former treatment were paraffin embedded 24 h after fixation. Staining for mKC (KC Rabbit Polyclonal Ab; BioVision) was performed on paraffin-embedded tissue from gd9- or gd15-treated and control-matched samples as previously described (29). F4/80$^+$ (MCA497R rat and mouse Ag; Serotec) cells were detected using paraffin-embedded tissue as described previously (30). Gr-1 (purified rat anti-mouse Ly6G and Ly6C; BD Biosciences) staining was performed on frozen gd9 and gd15 tissue cut into 10-μm sections as described previously (31).

Statistical analysis

Statistical significance of pregnancy outcomes was examined using the one-way ANOVA method. All experiments where flow cytometry plots were analyzed for n = 3 or more animals per condition and significance was assessed via the t test. Data are expressed as means ± SD. A p ≤ 0.05 was considered to be statistically significant.

Results

CpG ODN treatment induces fetal resorption and preterm birth in IL-10$^{-/-}$ mice

We studied the effect of CpG ODN treatment on pregnancy in either a fetal resorption or preterm birth model using C57BL/6 mice. The CpG ODN motif, CpG 1826, used in these studies has been widely used to trigger B or T cell-specific immunity (32, 33). To assess the ability of CpG ODN to induce fetal resorption, we injected i.p. varying doses of CpG ODN in IL-10$^{-/-}$ or WT mice on gd6. We initially tested a dose range from 5 to 400 μg/dam and found that the 25-μg dose was optimal in IL-10$^{-/-}$ mice to induce complete resorption of uterine horns. At the dose of 100 μg/dam or higher, we observed maternal wasting in IL-10$^{-/-}$ mice. As Fig. 1A demonstrates, fetal resorption was consistently observed in IL-10$^{-/-}$ mice in numerous matings (n = 37) at the 25-μg/dam dose. In contrast, no negative pregnancy effects were observed at this dose in WT mice (n = 8) as they maintained pregnancy to term (~20 days) and delivered healthy pups.

Next, we aimed to find a dose of CpG ODN that caused a negative pregnancy outcome in WT mice in response to gd6 administration. A range of doses up to 250 μg/dam did not exert any adverse consequences on pregnancy outcome or gestational length. However, at a dose of 400 μg/dam, a significant number of pups (43%) were born at term with cranial and distal limb malformations (Fig. 1C). These results are consistent with previously published data demonstrating similar deformities to pups born to dams treated with 300 μg of CpG ODN (19).
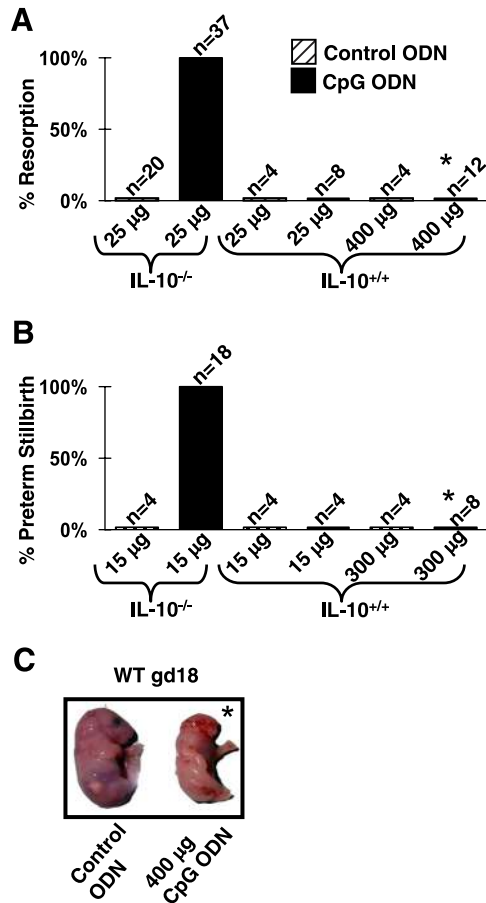
FIGURE 1. Dose-dependent CpG ODN-mediated induction of fetal resorption and preterm birth in WT or IL-10$^{-/-}$ mice. CpG or control ODN was injected i.p. in WT or IL-10$^{-/-}$ mice after visualization of a vaginal plug on gd0. *A*, Fetal resorption in uterine horns from IL-10$^{-/-}$ or WT mice was assessed visually on gd9 and mice were injected with CpG or control ODN on gd6. Twenty-five micrograms of CpG ODN induced full resorption of uterine horns in IL-10$^{-/-}$ mice ($n = 37$), whereas control ODN failed to elicit this pathology ($n = 20$). WT mice did not respond to 25 μg of CpG ODN nor control ODN. *B*, gd14 i.p. injection of 15 μg of CpG ODN induced preterm birth of stillborn pups within 24–48 h after injection in IL-10$^{-/-}$ mice ($n = 15$). Control ODN-treated IL-10$^{-/-}$ mice did not experience preterm delivery ($n = 4$). WT mice at this dose did not experience any preterm birth in the control ODN condition ($n = 4$) or CpG ODN condition ($n = 4$). *C*, In WT mice, a dose of 400 μg of CpG ODN given i.p. on gd6 caused cranial-facial and distal limb malformations, denoted by *, in 43% of pups born at term ($n = 12$). Similarly, a dose of 300 μg of CpG ODN in WT mice given i.p. on gd14 resulted in pups born at term with similar malformations ($n = 8$). WT mice treated with control ODN at these doses did not display teratogenic effects.

We have previously shown that LPS administered to IL-10$^{-/-}$ and WT mice on gd14 induces preterm birth on gd17, albeit at 20-fold higher doses in WT mice (10). For preterm birth outcomes in response to CpG ODN administration, a similar approach was used. CpG ODN was administered i.p. on gd14 and mice were checked twice daily for preterm birth of newborns. As shown in Fig. 1*B*, IL-10$^{-/-}$ mice ($n = 18$) consistently delivered stillborn pups at a dose of 15 μg/dam within 24–48 h of injection. Lower doses of CpG ODN failed to induce preterm delivery. Similar to fetal resorption observations, WT mice ($n = 4$) failed to experience any negative consequences of CpG ODN administration at a comparable or higher dose in the range of 300 μg/dam ($n = 8$), except for deformities at higher doses similar to that shown in Fig. 1*C*.
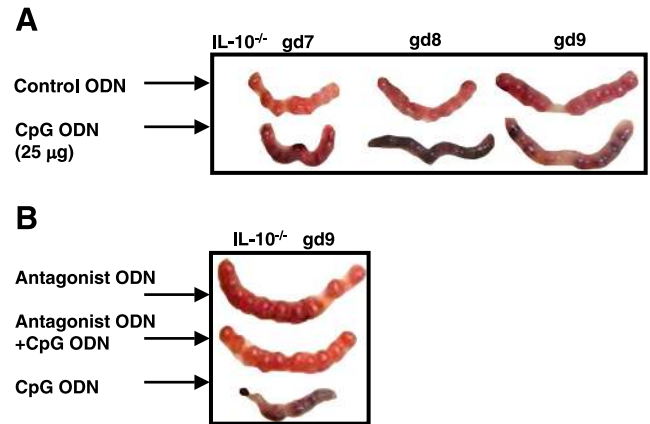

FIGURE 2. CpG ODN-induced fetal resorption in IL-10$^{-/-}$ mice occurs with rapid kinetics and is TLR9 dependent. *A*, Representative uterine horns of control and CpG ODN-treated IL-10$^{-/-}$ mice harvested on gd7, gd8, and gd9 represent multiple experiments of kinetic evaluation on the insult of placental pathologies. *B*, Representative uterine horns harvested on gd9 from IL-10$^{-/-}$ mice treated on gd6 with antagonist ODN 2088 (50 μg; *top panel*), antagonist ODN (50 μg) plus stimulatory CpG ODN (25 μg; *middle panel*), and CpG ODN alone (*bottom panel*) are shown. Data demonstrate antagonistic binding of antagonist ODN to TLR9 prevented fetal resorption ($n = 4$ animals/treatment).

Regarding fetal resorption in IL-10$^{-/-}$ mice, we noted that effects were rapid with severe uteroplacental pathology at 25 μg of CpG ODN (Fig. 1*A*). To characterize the kinetics and general pathology in IL-10$^{-/-}$ mice in response to CpG ODN administration, we visually assessed fetal resorption from gd7 through gd9. Fig. 2*A* demonstrates fetal resorption at 25 μg of CpG ODN as observed in uterine horns harvested as early as gd7 and the placental pathology appeared to increase in severity on gd8 and gd9. In contrast, control ODN-treated mice did not experience fetal resorption.

CpG ODN-mediated effects on pregnancy outcome are TLR9 dependent

CpG ODN 1826 is a promiscuous molecule which may signal not just through TLR9, but also through an extracellular receptor (34, 35). Thus, we assessed whether negative pregnancy outcomes in IL-10$^{-/-}$ mice were due to direct TLR9 stimulation. To address this issue, we used CpG ODN 2088 (antagonist ODN), an ODN sequence which binds intracellular TLR9 with high affinity but does not induce downstream stimulation of the TLR pathway (36–38). Antagonist ODN injected on gd6 did not induce any pathology in placental units harvested on gd9 (Fig. 2*B*). Importantly, mice treated with antagonist ODN when allowed to deliver gave birth to healthy litters at term. Antagonist ODN, when used with pathogenic CpG ODN at a 4:1 or 2:1 ratio, blocked fetal resorption compared with CpG ODN alone as demonstrated by normal placental units (Fig. 2*B*). If allowed to deliver, antagonist ODN plus CpG ODN-treated mice gave birth to healthy pups. These results demonstrate that antagonist ODN was able to successfully blunt the TLR9 receptor-mediated signaling and displace the binding of CpG ODN at a dose ratio as low as 2:1 as demonstrated by lack of resorption on gd9.

CpG ODN administration in IL-10$^{-/-}$ mice results in amplification and placental migration of uterine macrophages and neutrophils

In normal pregnancy, uNK cells, macrophages, and low numbers of T cells, but not Gr-1$^+$CD11b$^+$ cells, are normally detected in
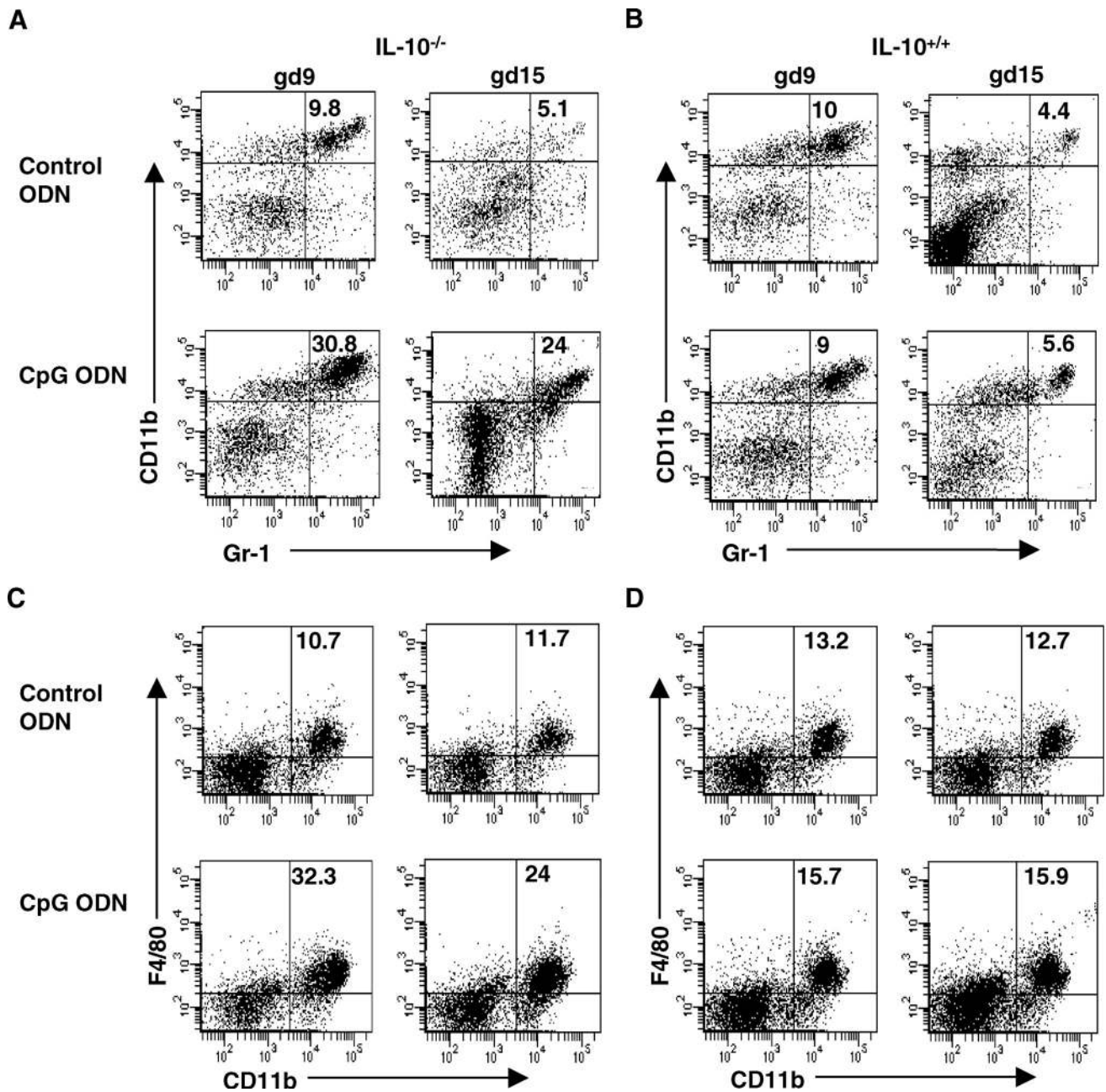
FIGURE 3. CD11b⁺Gr-1⁺ and CD11b⁺F4/80⁺ uterine cell populations amplify in response to CpG ODN in IL-10⁻/⁻, but not WT mice. Single-cell suspensions of UMGC populations were isolated from IL10⁻/⁻ (*A* and *C*) or WT (*B* and *D*) mice on gd9 or gd15 after treatment with control or CpG ODN. Cells were gated on CD45⁺ populations for CD11b⁺Gr-1⁺ (*A* and *B*) and CD11b⁺F4/80⁺ (*C* and *D*); data shown are representative of multiple experiments using four animals per condition. *A*, IL-10⁻/⁻ mice showed a significant increase in the CD11b⁺Gr-1⁺ population on gd9 and gd15, $p < 0.05$. *B*, WT mice under similar conditions did not show any significant changes in this population. *C*, IL-10⁻/⁻ mice showed a significant increase in the CD11b⁺F4/80⁺ cell population on gd9 and gd15, $p < 0.05$, compared with control ODN-treated mice. *D*, WT mice under similar conditions did not show any significant changes in this population.

the pregnant mouse uterus by gd7 (4, 39, 40). These cells remain localized to the maternal side of uteroplacental tissue within the mesometrial triangle and decidua basalis. However, it is not yet clear whether these uterine immune cells acquire a cytotoxic phenotype and migrate to the placental zone to cause local damage. In this regard, we have recently shown for the first time that uNK cells are indeed activated in response to LPS administration and cause apoptosis in the placental region (10). It is possible that severe and rapid pathology in CpG ODN-treated mice (Figs. 1 and 2*A*) may be programmed by the mechanisms of cellular activation and placental injury.

There is abundant evidence in nonpregnant mice that CpG ODN treatment leads to activation of dendritic cells (41). We prepared single-cell suspensions of CD45⁺ uterine mononuclear and granular cells as described in *Materials and Methods* and utilized flow cytometry to probe for the presence of CD11c⁺ (dendritic cells), CD11b⁺Gr-1⁺ (neutrophils), CD11b⁺F4/80⁺ (macrophages), or NK1.1⁺CD3⁻ (uNK cells) in IL-10⁻/⁻ and WT mice treated or untreated with CpG ODN. In the case of fetal resorption, we harvested uterine tissue and spleen on gd8 and 9, whereas for the preterm birth setting, we harvested uterine tissue and spleen 24 h after CpG ODN injection on gd15. Surprisingly, we did not
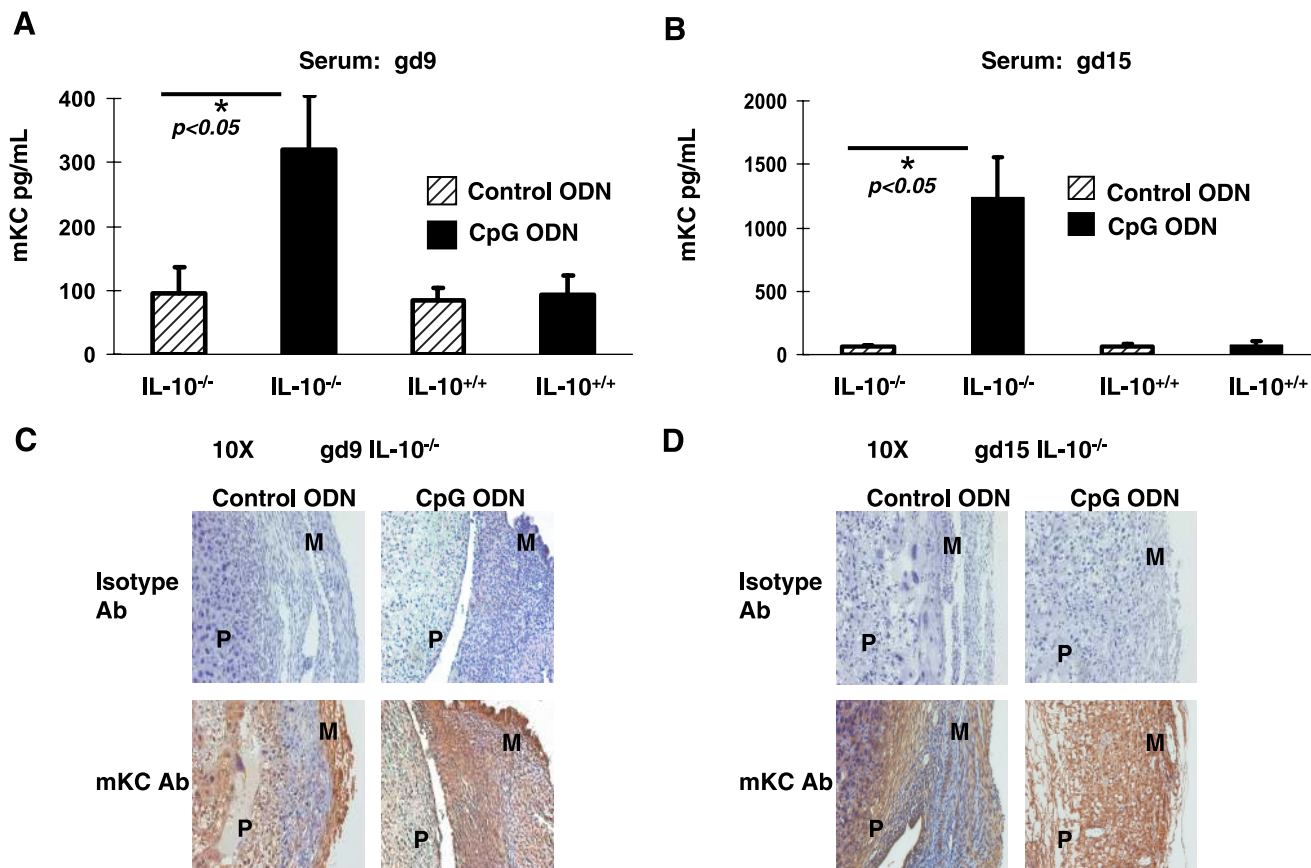
FIGURE 4. CpG ODN treatment leads to elevated production of mKC in IL-10$^{-/-}$ mice. mKC was measured in sera collected from IL-10$^{-/-}$ or WT mice on gd9 (*A*) or gd15 (*B*). Data represent average values from nine different serum samples. IL-10$^{-/-}$ mice (■) showed a significant increase in mKC levels above control ODN-treated mice (▨) on gd9 (*A*) and gd15 (*B*); ∗, $p < 0.05$. *C* and *D*, mKC was evaluated by immunohistochemistry done on uteroplacental tissue collected from control or CpG ODN-treated IL-10$^{-/-}$ mice. A marked increase in mKC protein was observed in CpG ODN-treated uterine tissue compared with control ODN-treated tissue on gd9 (*C*) and gd15 (*D*). M, Demarcates the mesometrial triangle, whereas P indicates the placental region.

see any changes in the dendritic cell populations of IL-10$^{-/-}$ or WT mice treated with 25 μg of CpG ODN on gd6 (data not shown).

Interestingly, analysis of gd8 and 9 uterine mononuclear and granular cells from CpG ODN-treated IL-10$^{-/-}$ mice showed a significant increase in the CD11b$^+$Gr-1$^+$ cellular population compared with vehicle-treated mice (9.3 ± 2.5 to 28.8 ± 4.4%; Fig. 3*A*). Similarly, we observed an increase in the CD11b$^+$GR1$^+$ cellular population in IL-10$^{-/-}$ mice under preterm birth conditions when analyzed on gd15 (6 ± 1.4 to 23.7 ± 3.5%; Fig. 3*A*). A simultaneous increase occurred in CD11b$^+$F4/80$^+$ populations. When analyzed on gd8 and 9, this population increased from 11.1 ± 0.9% to 35.0 ± 4.0% and a similar increase occurred in the preterm birth condition, 9.5 ± 3.1% to 25 ± 2.6% (Fig. 3*C*). At the doses used to induce fetal resorption or preterm birth in IL-10$^{-/-}$ mice, we did not observe any significant changes in either of these cellular populations in WT mice (Fig. 3, *B* and *D*).

Analysis of uNK cells revealed a slight increase in NK1.1$^+$ CD3$^-$ cells in CD45$^+$ mononuclear and granular cells from gd8 and 9 and gd15 tissues from IL-10$^{-/-}$ but not WT mice. However, depletion of uNK cells using anti-asialo GM1 Ab proved ineffective in rescuing fetal resorption or preterm birth in IL-10$^{-/-}$ mice treated with CpG ODN (data not shown). Thus, we focused on the role of macrophages and neutrophils in adverse pregnancy outcomes because these cells were highly amplified in response to CpG ODN treatment.

mKC is significantly induced in CpG ODN-treated IL-10$^{-/-}$ mice

We addressed the possibility that a suitable chemokine was induced in response to CpG ODN treatment in IL-10$^{-/-}$ mice that led to the unscheduled recruitment and amplification of granulocyte and monocyte (CD11b$^+$Gr-1$^+$, or CD11b$^+$F4/80$^+$) cellular populations. Initial screening was done for serum levels of MIP-1α, MIP-2, and mKC using chemokine-specific ELISAs. No significant changes were observed for MIP-1α or MIP-2 in serum samples from control ODN or CpG ODN-treated mice (data not shown). However, mKC, the mouse homologue of human IL-8 and a known chemoattractant of macrophages and neutrophils (42, 43), was markedly increased in samples from CpG ODN-treated IL-10$^{-/-}$ but not WT mice. The mKC levels in sera collected on gd9 from IL-10$^{-/-}$ mice averaged 94.3 ± 42.5 pg/ml in control ODN-treated mice and increased to an average of 319.1 ± 85.7 pg/ml in CpG ODN-treated mice, demonstrating a significant difference (Fig. 4*A*). Under identical conditions, no significant differences were observed in WT mice (Fig. 4*A*). Sera collected from gd15 IL-10$^{-/-}$ mice showed larger increases in mKC levels from an average of 63.4 ± 7.4 pg/ml in control animals ($n = 9$) to an average of 1242.9 ± 311.2 pg/ml in CpG ODN-treated animals ($n = 9$) with no significant changes in WT mice (Fig. 4*B*). IL-8 has been shown to be intrinsically produced at physiological levels by human uNK cells and it has been proposed that this chemokine
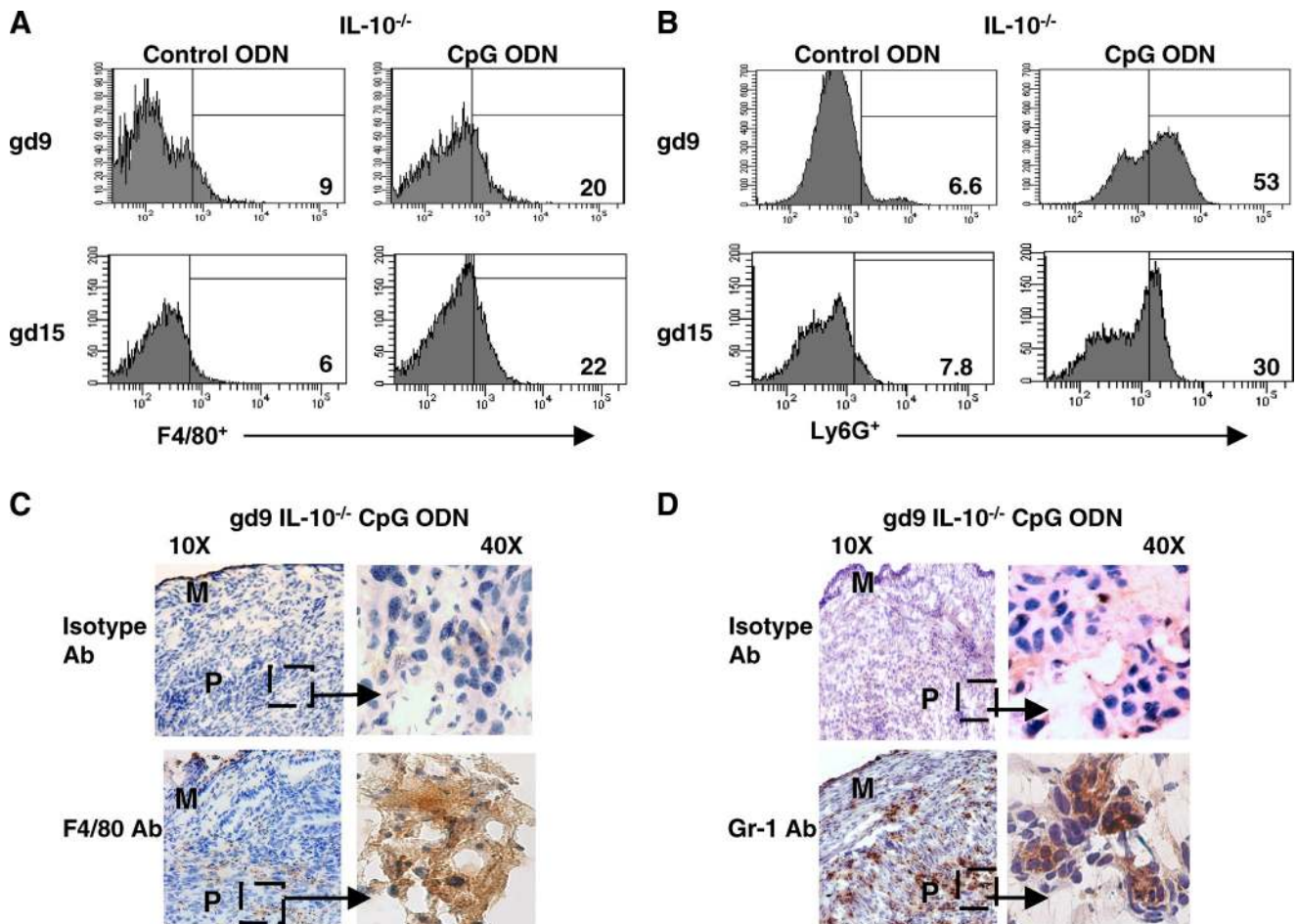
FIGURE 5. Macrophages and neutrophils migrate into the placental zone in response to CpG ODN in IL-10$^{-/-}$ mice. *A* and *B*, UMGC were harvested into single-cell suspensions from control or CpG ODN-treated IL-10$^{-/-}$ mice on gd9 and gd15. Histograms were gated from CD45$^+$ cells for F4/80$^+$ (*A*) or Ly6G$^+$ (*B*) cells. Histograms are representative of data from multiple experiments using four animals per condition. *A*, IL-10$^{-/-}$ mice showed a significant increase in F4/80$^+$ cells on gd9 and gd15 compared with control ODN-treated mice, $p < 0.05$. *B*, Similarly, IL-10$^{-/-}$ mice showed a significant increase in Ly6G$^+$ cells on gd9 and gd15 compared with control ODN-treated mice, $p < 0.05$. *C* and *D*, F4/80$^+$ and Gr-1$^+$ cells were evaluated by immunohistochemistry done on uteroplacental tissue collected on gd9 from CpG ODN-treated IL-10$^{-/-}$ mice. The presence of F4/80$^+$ (*C*) and Gr-1$^+$ (*D*) cells migrating from the myometrium and into the developing placental zone on gd9 in response to CpG ODN was observed. M, Demarcates the mesometrial triangle, whereas P indicates the placental region.

might be involved in recruitment of invading trophoblasts or macrophages for placental growth (6). We hypothesize that increased levels of mKC in response to CpG ODN motifs are responsible for the increased presence of CD11b$^+$Gr-1$^+$ and CD11b$^+$F4/80$^+$ cells in the uterine microenvironment.

Although an increase in serum mKC was observed, we wanted to determine that this protein was also produced locally at the maternal-fetal interface in response to CpG ODN. We performed mKC-specific immunostaining on paraffin-embedded sections of CpG ODN-treated uteroplacental tissue from IL-10$^{-/-}$ mice obtained on gd9 or gd15. Although tissue from control ODN-treated mice showed basal mKC staining in the mesometrial and developing placental regions on gd9 or gd15 (Fig. 4, *C* and *D*), CpG ODN treatment resulted in intense staining throughout the tissue organization collected from gd9 or gd15. Isotype control Ab failed to stain any specific regions of tissue sections (Fig. 4, *C* and *D*).

CpG ODN-activated Gr-1$^+$ and F4/80$^+$ uterine cells migrate to the placenta in IL-10$^{-/-}$ mice

As mentioned earlier, uterine immune cells remain localized to the maternal part of uteroplacental tissue (3, 5, 9, 40). In this study, we tested the hypothesis that CpG ODN treatment imparts migration

of Gr-1$^+$ and F4/80$^+$ uterine cells to the placenta leading to adverse pregnancy outcomes. Gr-1$^+$ populations can be indicative of macrophages or neutrophils, thus we first aimed to specify the contribution of each of these particular cell types at the placental level. From tissues harvested on gd9 and gd15, we isolated mononuclear and granular cells and analyzed the CD45$^+$ population by FACS for macrophage or neutrophil markers F4/80 and Ly6G, respectively. F4/80 positivity was markedly increased in both the fetal resorption (10.5 ± 1.3 to $21.5 \pm 1.3\%$) and preterm birth conditions over control levels (6.5 ± 1.3 to $21.0 \pm 3.1\%$; Fig. 5*A*). We next examined whether F4/80$^+$ cells migrated to the placental zone. Uteroplacental tissue from gd9 was processed for immunohistochemical analysis of F4/80 positive staining (see *Materials and Methods*). As shown in Fig. 5*C*, no significant staining was observed with isotype Ab in CpG ODN-treated tissue. However, there was an abundance of F4/80$^+$ cells that were found not only in the mesometrial zone but also in the placental zone at gd9 (Fig. 5*C*). Control ODN-treated tissue showed low levels of F4/80$^+$ cells localized only to mesometrial zone (data not shown).

We next aimed to delineate the specific presence of neutrophils in uteroplacental tissue. As shown in Fig. 3, Gr-1$^+$ cells increased significantly in the CD45$^+$ uterine population from
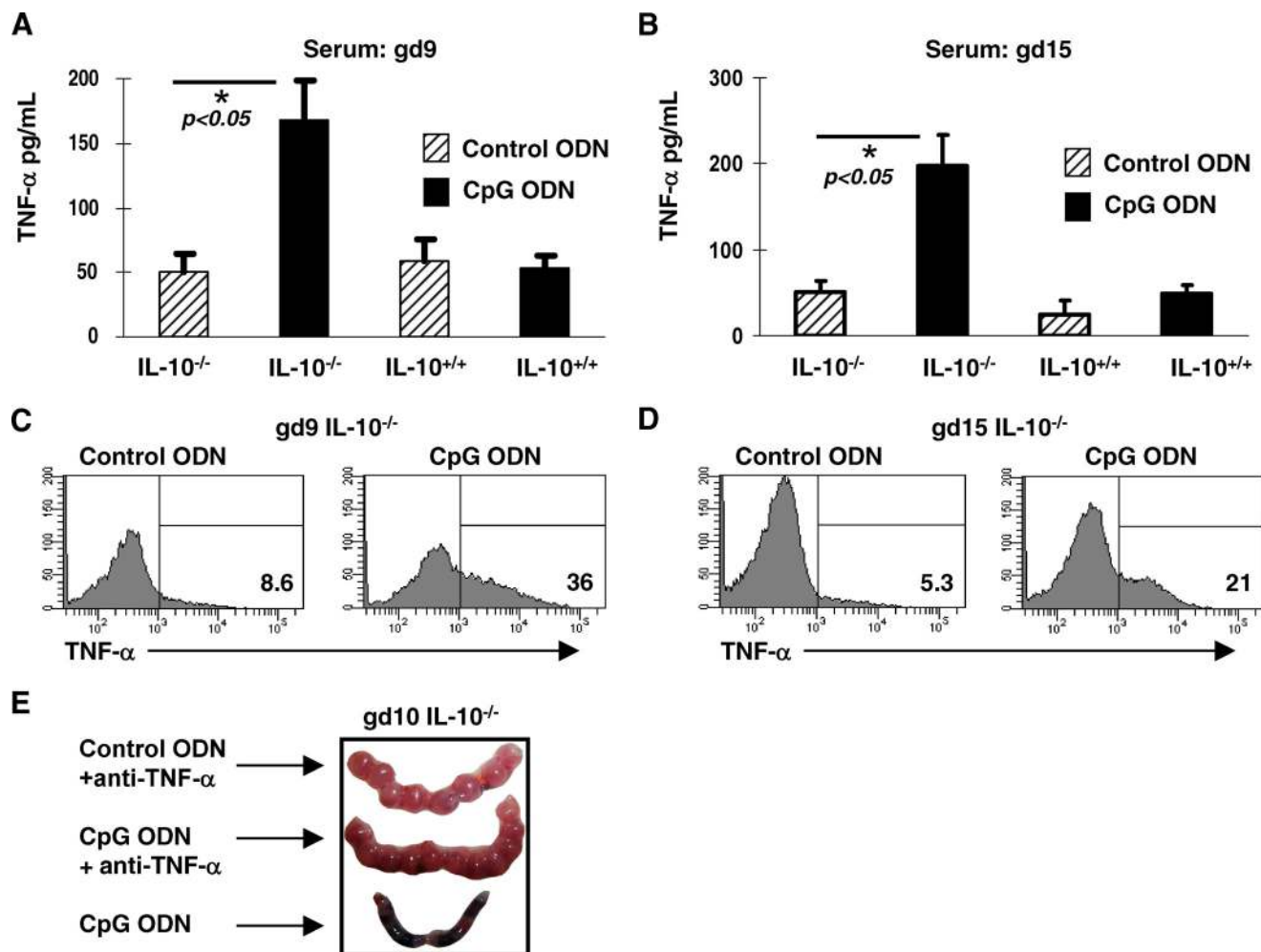
FIGURE 6. TNF-α is the essential cytotoxic factor leading to fetal resorption or preterm birth in response to CpG ODN in IL-10$^{-/-}$ mice. TNF-α was measured in sera collected from IL-10$^{-/-}$ or WT mice on gd9 (*A*) or gd15 (*B*). Data represent average values from nine different serum samples. IL-10$^{-/-}$ mice (■) showed a significant increase in TNF-α levels above control ODN-treated mice (▨) on gd9 (*A*) and gd15 (*B*); *, $p < 0.05$. *C* and *D*, UMGC were collected on gd9 (*C*) or gd15 (*D*) from IL-10$^{-/-}$ mice treated with control or CpG ODN to probe for the presence of TNF-α. Histograms are gated on CD45^{+} cells and are representative of data from multiple experiments using four animals per condition. IL-10$^{-/-}$ mice showed a significant increase in TNF-α $^{+}$ cells on gd9 (*C*) and gd15 (*D*) compared with control ODN-treated mice, $p < 0.05$. *E*, anti-TNF-α mAb Ab, given i.p. on gd5 and 7, was used to neutralize TNF-α activity induced by CpG ODN given on gd6. Data are representative of gd10 uterine horns treated with control ODN + anti-TNF-α (*top panel*), CpG ODN + anti-TNF-α (*middle panel*), or CpG ODN alone (*bottom panel*). Data represent multiple experiments using four animals per condition.

CpG ODN-treated IL-10$^{-/-}$ mice. The Gr-1 receptor is composed of the Ly6G and Ly6C subreceptors (44). Although it is commonly accepted in the literature that Gr-1-positive cells are representative of neutrophils, we assessed these cells using the Ly6G Ab. As shown in Fig. 5*B*, Ly6G^{+} cells increased significantly from control levels in both gd9 (5.7 ± 1.7 to 53.2 ± 7.1%) and gd15 (7.8 ± 3.0 to 28.3 ± 6.5%) tissues. Immunohistochemical analysis further demonstrated migration of Gr-1^{+} cells well into the placental zone in tissue harvested on gd9 from CpG ODN- treated IL-10$^{-/-}$ mice (Fig. 5*D*). Taken together, these data imply that migration of macrophages and neutrophils to the placenta may lead to pathological outcomes.

TNF-α functions as the regulator of CpG ODN-mediated pregnancy loss

As discussed above, mKC was detected at high levels in serum of CpG ODN-treated IL-10$^{-/-}$ mice, suggesting that it could contribute to pregnancy complications. However, experiments involving mKC neutralization did not result in rescue of pregnancy (data

not shown). We hypothesized that a distinct cytotoxic factor(s) was produced by macrophages and/or neutrophils that induced adverse pregnancy outcomes in IL-10$^{-/-}$ mice. CpG ODN is known to induce the expression of a variety of cytotoxic proteins, including IFN-γ, TNF- α, and IL-12 (45). We measured the concentration of IFN-γ, IL-12, and TNF-α in serum samples collected on gd9 from mice treated with 25 μg of CpG ODN or control ODN on gd6 and in gd15 serum from mice treated with 15 μg of CpG ODN or control ODN on gd14. In both the fetal resorption (50.1 ± 15.0 to 168 ± 30.9 pg/ml) (Fig. 6A) and preterm birth conditions (51.0 ± 11.9 to 196.9 ± 36.1 pg/ml; Fig. 6*B*), we noted a significant increase in serum TNF-α levels in CpG ODN-treated IL-10$^{-/-}$ mice, but not in CpG ODN-treated WT mice. No significant differences were observed for IFN-γ and IL-12 between treated or untreated IL-10$^{-/-}$ or WT mice (data not shown).

Due to the increased levels of this toxic cytokine in serum in response to CpG ODN, we aimed to determine whether TNF-α was being produced within the uterine tissue of CpG ODN-treated IL-10$^{-/-}$ mice. Uterine monocytes and granulocyte populations

Table I. *Rescue of CpG ODN-induced preterm birth in IL-10$^{-/-}$ mice*

Strain	Treatment	n	gd Birth[a]	p
C57BL/6 IL-10$^{-/-}$	CpG ODN + isotype Ab[b]	3	15.5 ± 0.5	
	Control ODN + anti-TNF-α	3	20.0 ± 1.0	
	CpG ODN + anti-TNF-α	4	20.6 ± 0.8	<0.001[c]
	CpG ODN + isotype Ab[d]	3	15.2 ± 0.3	
	Control ODN + anti-F4/80	3	19.7 ± 1.1	
	CpG ODN + anti-F4/80	4	20.1 ± 0.8	<0.001

[a] gd of birth was assessed visually by the presence of live or dead pups delivered after gd14 treatment.
[b] Isotype Ab paired to anti-TNF-α administration is listed in *Materials and Methods*.
[c] Value of p compares significance of gd of birth between CpG ODN + Ab to CpG ODN + isotype Ab.
[d] Isotype Ab paired to anti-F4/80 administration is listed in *Materials and Methods*.

were isolated and intracellular staining for TNF-α was performed as described in *Materials and Methods*. Uterine CD45$^+$ cells from CpG ODN-treated tissue showed a marked increase in intracellular TNF-α production compared with those from control ODN-treated tissue from gd9 (8.25 ± 1.7 to 40.5 ± 8.3%; Fig. 6C). Similar results were obtained from uterine cells isolated from gd15 tissue (6.25 ± 2.0 to 21.5 ± 3.3%; Fig. 6D).

Since we noted a significant increase in TNF-α both in serum and in uterine CD45$^+$ cells in CpG ODN-treated IL-10$^{-/-}$ mice, we aimed to determine whether this cytokine played a critical role in adverse pregnancy outcomes. We used a neutralizing Ab for in vivo inactivation of TNF-α. In the context of early pregnancy loss, we injected anti-TNF-α Ab on gd5 and gd7 in combination with a CpG ODN injection on gd6. First, we noted healthy litters were born at term in mice treated at the aforementioned time points. Correspondingly, mice treated with CpG ODN on gd6 showed intact fetal-placental units on gd10 in response to anti-TNF-α

treatment (Fig. 6E). Similarly, mice treated with CpG ODN on gd14 gave birth to healthy litters at term when given injections of anti-TNF-α Ab on gd13 and 15 (Table I).

Gr-1$^+$ cellular depletion in IL-10$^{-/-}$ mice does not lead to pregnancy rescue or reduced TNF-α production

We sought to examine the cellular origin of TNF-α and the role that CD11b$^+$Gr-1$^+$ populations played in CpG ODN-induced fetal demise in IL-10$^{-/-}$ mice. We first assessed the effects of depletion of Gr-1$^+$ cells. We used an anti-Gr-1$^+$ Ab which was administered i.p. in one dose on gd5 with a CpG ODN injection on gd6 followed by euthanization of animals on gd9 to determine whether rescue from fetal resorption ensued. As shown in Fig. 7A, anti-Gr-1$^+$ Ab treatment depleted Gr-1$^+$ cells in CpG ODN-treated IL-10$^{-/-}$ mice. However, this event was not associated with the depletion of a CD45$^+$TNF-α$^+$-producing population as assessed simultaneously by intracellular FACS staining (Fig. 7A). In addition, depletion of Gr-1$^+$ cells did not rescue pregnancy. These observations suggest that the large infiltrates of Ly6G$^+$Gr-1$^+$ cells in response to CpG ODN treatment (Fig. 5, B and D) play a secondary role in induction of CpG ODN-mediated fetal resorption or preterm birth.

Evidence of respiratory burst in uterine Gr-1$^+$CD11b$^+$ cells from CpG ODN-treated IL-10$^{-/-}$ mice

Although uterine Gr-1$^+$ cells did not produce TNF-α (Fig. 7A) and their depletion did not lead to pregnancy rescue, it is still not clear whether these cells were activated and harbor a cytotoxic phenotype. In this regard, we examined production of ROS by Gr-1$^+$ uterine cells because it is a specific phenotype of these cells upon activation (46, 47). To assess the production of ROS, we used DHR in flow cytometric analysis. This molecule increases its fluorescent intensity upon oxygenation and has recently been used to
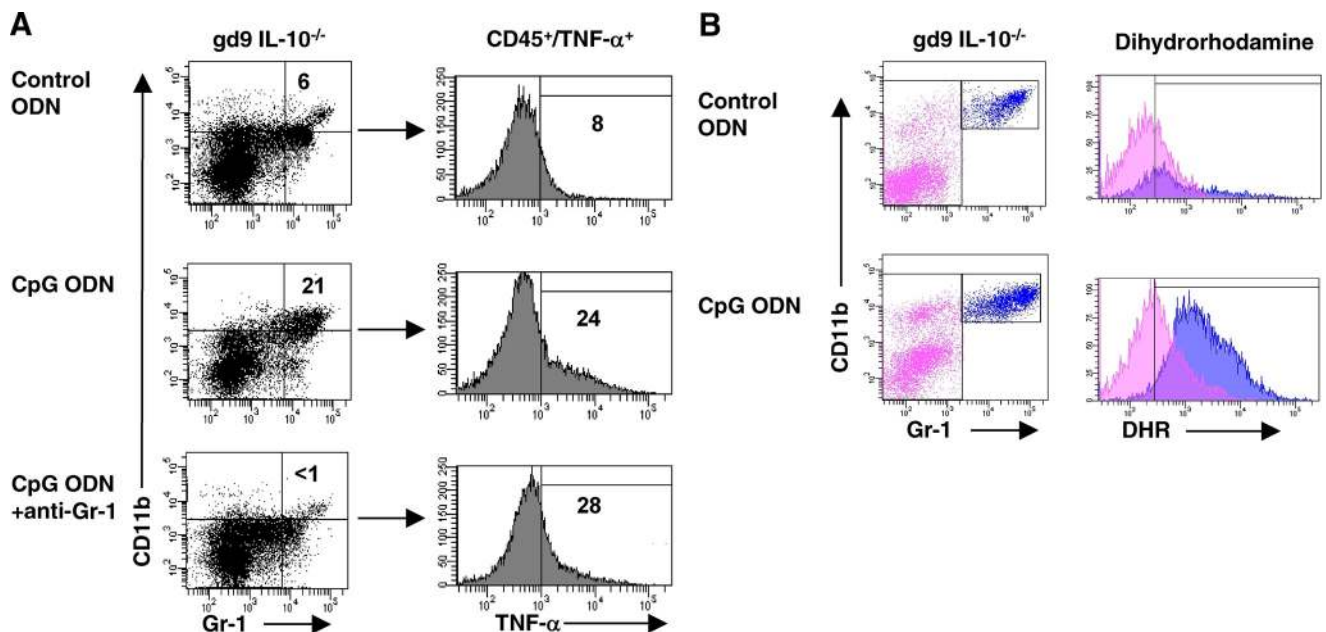
FIGURE 7. Gr-1 depletion does not rescue CpG ODN-mediated negative fetal outcomes in IL-10$^{-/-}$ mice, but Gr-1$^+$ cells actively produce ROS. *A*, Anti-Gr-1 mAb was used to deplete Gr-1$^+$ uterine cells. Dot plots are gated on CD45$^+$ cells for CD11b$^+$Gr-1$^+$ populations. Data represent multiple experiments using four animals per condition. Although Gr-1$^+$ cells were successfully depleted below control levels, no rescue of pregnancy resulted. TNF-α from these CD45$^+$ cells was evaluated and histograms show that the presence of TNF-α under the given conditions was not abrogated. *B*, A role for the increasing CD11b$^+$Gr-1$^+$ populations in response to CpG ODN was evaluated via DHR fluorescence. The two gates on dot plots correspond to the cell populations displayed in the histograms: pink is CD45$^+$Gr-1$^+$ and blue is CD45$^+$Gr-1$^+$CD11b^{high}. Data are representative of results from gd9 control or CpG ODN-treated IL-10$^{-/-}$ mice. Control ODN-treated samples (*top panel*) or CpG ODN-treated samples (*bottom panel*) show a mean fluorescent intensity shift of DHR in the blue population of CpG ODN-treated animals only, indicative of respiratory burst.
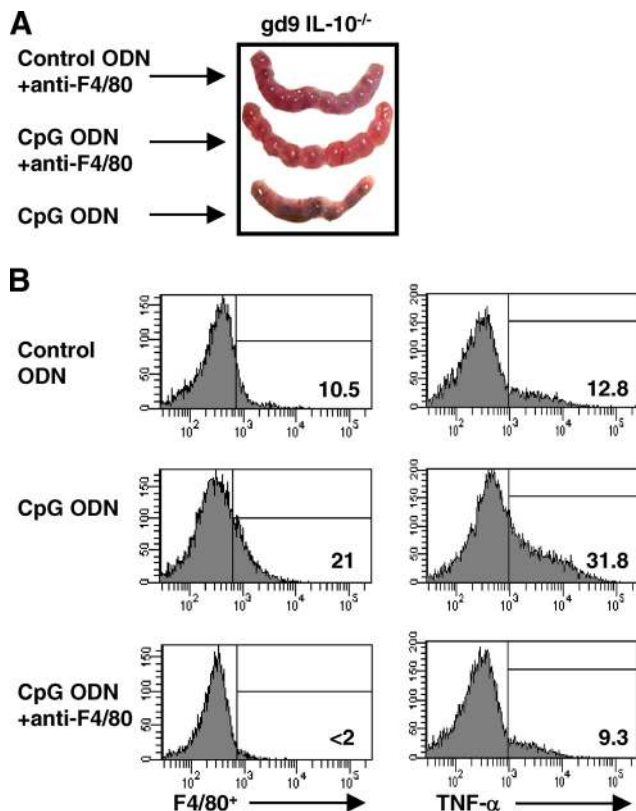
FIGURE 8. Macrophage depletion abrogates CpG ODN-mediated negative fetal outcomes and diminishes TNF-α activity. *A*, Intact uterine horns on gd9 demonstrate that anti-F4/80 mAb successfully rescued fetoplacental units from fetal resorption. *Top panel* is control ODN + anti-F4/80 mAb, *middle panel* is CpG ODN + anti-F4/80 mAb, and *bottom panel* shows fetal resorption from CpG ODN alone. Data are representative of multiple experiments using three animals per condition. *B*, UMGC from gd9 are gated on CD45$^+$ cells and show depletion of F4/80$^+$ cells (*left*) coupled to a lack of TNF-α^+ (*right*) production. TNF-α increase was significant over control levels only in the CpG ODN-alone treatment condition, $p < 0.05$. Histograms are representative of multiple experiments using three animals per condition.

measure production of ROS in several studies (31). CD45$^+$CD11b$^+$ Gr-1$^+$ cells were typed from gd9 or gd15 uteroplacental tissue from control ODN- or CpG ODN-treated IL-10$^{-/-}$ mice and stained simultaneously with DHR as described in *Materials and Methods*. Uterine CD45$^+$CD11b$^+$Gr-1$^+$cellular populations from CpG ODN-treated tissue harvested on gd9 (Fig. 7*B*) or gd15 (data not shown) show a significant increase in DHR fluorescence, as calculated by an increase in mean fluorescent intensity compared with that seen in tissues from control ODN-treated mice. These data clearly suggest that uterine Gr-1$^+$ cells acquire an activated phenotype in CpG ODN-treated IL-10$^{-/-}$ mice as depicted by ROS production. However, since Gr-1$^+$ depletion did not rescue negative pregnancy outcomes in response to CpG ODN, ROS production by Gr-1$^+$ cells may cause placental cell death in conjunction with cytokines that may be produced by other activated uterine immune cells.

F4/80$^+$ cellular depletion abrogates TNF-α production in IL-10$^{-/-}$ mice leads to term pregnancy

We next examined the uterine cell type associated with TNF-α production to define the mechanism of fetal demise at a cellular level. Because Gr-1$^+$ cellular depletion proved inadequate as a means to rescue pregnancy, we examined the potential contribu-

tion of macrophages in CpG ODN-induced adverse pregnancy outcomes. In the fetal resorption setting, we injected an anti-F4/80 Ab i.p. on gd5 and gd7 with CpG ODN injection on gd6. For the preterm birth condition, the anti-F4/80 Ab was injected on gd13 before gd14 injection of CpG ODN. As shown in Fig. 8*A*, F4/80 Ab treatment rescued pregnancy because the fetoplacental units harvested on gd10 remained intact, and mice that were allowed to proceed to term delivered healthy litters (Table I). Similarly as is shown in Table I, preterm birth effects in response to CpG ODN were abrogated in response to anti-F4/80 Ab injection. To ensure that F4/80$^+$ cells were depleted, we analyzed CD45$^+$ uterine mononuclear and granular cell population by FACS for the presence of an F4/80$^+$ population. As shown in Fig. 8*B*, uterine F4/80$^+$ cells were successfully depleted below those of control levels. CpG ODN, however, amplified the proportional presence of F4/80$^+$ cells upward of 20%, similar to results shown in Figs. 3 and 5. Importantly, we assessed intracellular TNF-α production from CpG ODN-treated mice depleted or not depleted for F4/80$^+$ cells from gd9 uteroplacental tissues. In the F4/80$^+$-depleted mice, there was a lack of intracellular staining for TNF-α compared with levels seen in response to CpG ODN alone (Fig. 8*B*). These data suggest a causative role of uterine macrophages in inducing adverse pregnancy outcomes in CpG ODN-treated IL-10$^{-/-}$ mice.

Discussion

It is widely accepted that the innate immune system is essential as a dynamic factor that could be both protective and detrimental to the maternal-fetal stasis (3, 8–10). Although its role is poorly understood, the relative presence of the TLR system in the placental microenvironment further adds to this complexity. Growing evidence clearly suggests that TLR-mediated activation through endogenous signals may indeed provide pregnancy-compatible responses (12, 48). On the other hand, it is not yet fully understood how the TLR machinery will respond to external signals with origins from intrauterine infections and inflammation, particularly when coupled with intrinsic deficiencies in molecules that are critical to normal pregnancy outcome. Two such scenarios are the bacterial and viral DNA breakdown products represented by unmethylated CpG ODN motifs and dsRNA.

In this study, we have examined the gestational age-dependent consequences of CpG ODN administration in pregnant WT and IL-10$^{-/-}$ mice. We observed that when injected i.p. on gd6 or gd14, CpG ODN caused rapid fetal resorption or preterm stillbirth in IL-10$^{-/-}$ mice, respectively (Fig. 1). In contrast, a similar low dose or a 10-fold higher CpG ODN dose failed to exert any adverse pregnancy effects in WT mice. CpG ODN-mediated consequences in IL-10$^{-/-}$ mice were TLR9 specific as an antagonistic CpG ODN ligand-rescued pregnancy in response to pathogenic CpG ODN (Fig. 2*B*). These observations point to a protective role of IL-10 at the maternal-fetal interface when challenged with bacterial or viral pathogens that may give rise to CpG-like breakdown products.

Several key features were noted in pregnant IL-10$^{-/-}$ mice when challenged with the pathogenic CpG ODN motif. First, the induction of fetal resorption or preterm birth was rapid and severe (Fig. 2*A*). In comparison, WT mice only experienced teratogenic effects at a very high dose ($\sim$400 μg/dam) in a portion of the litter at term. Second, the functional presence of uterine CD11b$^+$F4/80$^+$ macrophages and CD11b$^+$Gr-1$^+$ neutrophils (Fig. 3), not CD11c$^+$ dendritic cells or NK1.1$^+$/CD3$^-$ NK cells, was significantly increased. This influx was critically associated with a drastic increase in serum and the local presence of mKC (Fig. 4). Uterine macrophages, not Gr-1$^+$ neutrophils, exhibited a significantly high

production of TNF-α (Fig. 8). Importantly, both cell types uncharacteristically migrated to the placental zone (Fig. 5). Finally, depletion of F4/80$^+$ cells (Fig. 8) or in vivo neutralization of TNF-α (Fig. 6E) in CpG-treated IL-10$^{-/-}$ mice blunted fetal resorption and preterm birth and rescued pregnancy to term (Table I).

It is important to mention that depletion of Gr-1$^+$ cells did not lead to rescue of pregnancy nor did it reduce the presence of TNF-α-producing uterine cells (Fig. 7). Thus, when encountered in an abortion- or preterm birth-prone environment such as IL-10 deficiency, TLR9-triggered cytotoxic activation of macrophages and TNF-α production has severe pathological effects on pregnancy. Neutrophils may influence pregnancy outcome mainly through production of ROS (Fig. 7). These results are important in light of the numerous reports on the association of bacterial and viral infections with early and late pregnancy loss in humans (1, 2, 49, 50). In connection with these data, recent cohort studies have demonstrated that women with abnormally low IL-10 production are more susceptible to systemic and intrauterine infections, leading to increased incidence of pregnancy loss (51–54).

TLR9, localized in intracellular compartments, is expressed in both innate and adaptive immune cells and has been shown to be present in uterine immune cells (11, 14, 15). Curiously, human placental explants did not show any response to CpG compared with agonists for other TLRs (12), suggesting that in humans the maternal immune cells are the major target for CpG-mediated effects. It is possible that TLR9 remains localized to the endoplasmic reticulum of the trophoblast in a nonfunctional form, whereas it becomes activated by localizing to and undergoing cleavage in endolysosomes in uterine macrophages and neutrophils (55, 56). TLR9 signaling has been shown to be essential for recruitment and activation of NK and dendritic cells in many settings of parasitic and bacterial infections (57). TLR9$^{-/-}$ mice have been shown to lack cytotoxic activation of these cells following infection with *Leishmania major* (58). Since we did not observe cytotoxic activation of uNK cells, it is possible that these cells behave differently in response to pathogenic TLR9 agonists than circulating NK cells.

Our findings of high levels of mKC are critical for implications toward understanding the balance between maternal and fetal health. IL-8 has been shown to be imperative for proper trophoblast cell invasion in humans (6). On the other hand, dysregulated production of this chemokine in response to a TLR9-mediated inflammatory insult could prove to be highly detrimental by way of the robust recruitment of cytotoxic macrophages and neutrophils.

We have shown an increased incidence of two cellular populations in response to CpG-mediated pathogens in IL-10$^{-/-}$ mice, namely, macrophages and neutrophils (Figs. 3 and 5). Although the response of these cells to this TLR9 ligand is widely expected (59, 60), this is the first time it has been documented in the context of pregnancy and the uterine microenvironment. We have elucidated novel mechanisms involving these two cell types as first responders to CpG-mediated inflammatory insult, and we have parsed apart their individual roles in this system. Importantly, we have linked the role of macrophages with the production of TNF-α in response to CpG challenge during pregnancy (Fig. 8). Based on our recent findings with other TLR ligands (Refs. 9 and 10; our unpublished observations), we propose that TNF-α is a common final product in response to a spectrum of TLR agonists that induce adverse pregnancy outcomes in response to systemic administration. As shown in Fig. 6 and Table I, neutralization of TNF-α resulted in rescue of pregnancy to term, suggesting that renewed focus should be assigned to the cellular producers of this cytotoxin in response to a particular TLR that is activated. An understanding of the cellular diversity of TNF-α production at the maternal-fetal interface may be essential in providing proper therapeutic interventions in the context of pregnancy complications.

Disclosures

The authors have no financial conflict of interest.

References

1. Goldenberg, R. L., J. C. Hauth, and W. W. Andrew. 2000. Intrauterine infection and preterm delivery. *N. Engl. J. Med.* 342: 1500–1507.
2. Romero, R., J. Espinoza, and M. Mazor. 2004. Can endometrial infection/inflammation explain implantation failure, spontaneous abortion, and preterm birth after in vitro fertilization? *Fertil. Steril.* 82: 799–804.
3. Moffett-King, A. 2002. Natural killer cells and pregnancy. *Nat. Rev. Immunol.* 2: 656–663.
4. Whitelaw, P. F., and B. A. Croy. 1996. Granulated lymphocytes of pregnancy. *Placenta* 17: 533–543.
5. Ain, R., L. N. Canham, and M. J. Soares. 2003. Gestational stage-dependent intrauterine trophoblast cell invasion in the rat and mouse: novel endocrine phenotype regulation. *Dev. Biol.* 260: 176–190.
6. Hanna, J., D. Goldman-Wohl, Y. Hamani, I. Avraham, C. Greenfield, S. Natanson-Yaron, D. Prus, L. Cohen-Daniel, T. I. Arnon, I. Manaster, et al. 2006. Decidual NK cells regulate key developmental processes at the human fetal-maternal interface. *Nat. Med.* 12: 1065–1074.
7. Kalkunte, S., C. O. Chichester, F. Gotsch, C. L. Sentman, R. Romero, and S. Sharma. 2008. Evolution of non-cytotoxic uterine natural killer cells. *Am. J. Reprod. Immunol.* 59: 425–432.
8. Kalkunte, S., T. F. Mselle, W. E. Norris, C. R. Wira, C. L. Sentman, and S. Sharma. 2009. VEGF C facilitates immune tolerance and endovascular activity of human uterine NK cells at the maternal-fetal interface. *J. Immunol.* 182: 4085–4092.
9. Murphy, S. P., L. D. Fast, N. N. Hanna, and S. Sharma. 2005. Uterine NK cells mediate inflammation-induced fetal demise in IL-10-null mice. *J. Immunol.* 175: 4084–4090.
10. Murphy, S. P., N. N. Hanna, L. D. Fast, S. K. Shaw, G. Berg, J. F. Padbury, R. Romero, and S. Sharma. 2009. Evidence for participation of uterine NK cells in the mechanisms responsible for spontaneous preterm labor and delivery. *Am. J. Obstet. Gynecol.* 200: 308e1–308e9.
11. Sentman, C. L., C. R. Wira, and M. Eriksson. 2007. NK cell function in the human female reproductive tract. *Am. J. Reprod. Immunol.* 57: 108–115.
12. Patni, S., L. P. Wynen, A. L. Seager, G. Morgan, J. O. White, and C. A. Thornton. 2009. Expression and Activity of Toll-like receptors 1–9 in the human term placenta and changes associated with labor at term. *Biol. Reprod.* 80: 243–248.
13. Krikun, G., C. J. Lockwood, V. M. Abrahams, G. Mor, M. Paidas, and S. Guller. 2007. Expression of Toll-like receptors in the human decidua. *Histol. Histopathol.* 22: 847–854.
14. Barton, G. M., and R. Medzhitov. 2002. Toll-like receptors and their ligands. *Curr. Top. Microbiol. Immunol.* 270: 81–92.
15. Uematsu, S., and S. Akira. 2006. Toll-like receptors and innate immunity. *J. Mol. Med.* 84: 712–725.
16. Trinchieri, G., and A. Sher. 2007. Cooperation of Toll-like receptor signals in innate immune defence. *Nat. Rev. Immunol.* 7: 179–190.
17. Krieg, A. M. 2002. CpG Motifs in bacterial DNA and their immune effects. *Annu. Rev. Immunol.* 20: 709–760.
18. Pedersen, G., L. Andresen, M. W. Matthiessen, J. Rask-Madsen, and J. Brynskov. 2005. Expression of Toll-like receptor 9 and response to bacterial CpG oligodeoxynucleotides in human intestinal epithelium. *Clin. Exp. Immunol.* 141: 298–306.
19. Prater, M. R., V. J. Johnson, D. R. Germolec, M. I. Luster, and S. D. Holladay. 2006. Maternal treatment with a high dose of CpG ODN during gestation alters fetal craniofacial and distal limb development in C57BL/6 mice. *Vaccine* 24: 263–271.
20. Ito, S., K. J. Ishii, H. Shirota, and D. M. Klinman. 2004. CpG oligodeoxynucleotides improve survival of pregnant and fetal mice following *Listeria monocytogenes* infection. *Infect. Immun.* 72: 354–358.
21. Carpentier, A. F., L. Chen, F. Maltonti, and J. Y. Delattre. 1999. Oligodeoxynucleotides containing CpG motifs can induce rejection of neuroblastoma in mice. *Cancer Res.* 59: 5429–5432.
22. Carpentier, A. F., J. Xie, K. Mokhtari, and J. Y. Delattre. 2000. Successful treatment of intracranial gliomas in rat by oligodeoxynucleotides containing CpG motifs. *Clin. Cancer Res.* 6: 2469–2473.
23. Meng, Y., A. F. Carpentier, L. Chen, G. Boisserie, J. M. Simon, J. J. Mazeron, and J. Y. Delattre. 2005. Successful combination of local CpG-ODN and radiotherapy in malignant glioma. *Int. J. Cancer* 116: 992–997.
24. Becker, Y. 2005. CpG ODNs treatments of HIV-1 infected patients may cause the decline of transmission in high risk populations: a review, hypothesis and implications. *Virus Genes* 30: 251–266.
25. Kline, J. N., and A. M. Krieg. 2008. Toll-like receptor 9 activation with CpG oligodeoxynucleotides for asthma therapy. *Drug News Perspect.* 21: 434–439.

26. Manegold, C., D. Gravenor, D. Woytowitz, J. Mezger, V. Hirsch, M. Al-Adhami, D. Readett, A. M. Krieg, and C. G. Leichman. 2008. Randomized phase II trial of Toll-like receptor 9 agonist oligodeoxynucleotide, PF-3512676, in combination with first-line taxane plus platinum chemotherapy for advanced stage non-small-cell lung cancer. *J. Clin. Oncol.* 26: 3979–3986.

27. Chaung, H. C. 2006. CpG oligodeoxynucleotides as DNA adjuvants in vertebrates and their applications in immunotherapy. *Int. Immunopharmacol.* 6: 1586–1596.

28. Jenkins, M., C. Parker, W. Tuo, B. Vinyard, and J. P. Dubey. 2004. Inclusion of CpG adjuvant with plasmid DNA coding for NcGRA7 improves protection against congenital neosporosis. *Infect. Immun.* 72: 1817–1819.

29. Roche, J. K., T. R. Keepers, L. K. Gross, R. M. Seaner, and T. G. Obrig. 2007. CXCL1/KC and CXCL2/MIP-2 are critical effectors and potential targets for therapy of *Escherichia coli* 0157:H7-associated renal inflammation. *Am. J. Pathol.* 170: 526–537.

30. Siewe, L., M. Bollati-Fogolin, C. Wickenhauser, T. Krieg, W. Muller, and A. Rogers. 2006. Interleukin-10 derived from macrophages and/or neutrophils regulates the inflammatory response to LPS but not the response to CpG DNA. *Eur. J. Immunol.* 36: 3248–3255.

31. Redecha, P., R. Tilley, M. Tencati, J. E. Salmon, D. Kirchhofer, N. Mackman, and G. Girardi. 2007. Tissue factor: a link between C5a and neutrophil activation in antiphospholipid antibody induced fetal injury. *Blood* 110: 2423–2431.

32. Ballas, Z. K., A. M. Krieg, T. Warren, W. Rasmussen, H. L. Davis, M. Waldschmidt, and G. J. Weiner. 2001. Divergent therapeutic and immunologic effect of oligodeoxynucleotides with distinct CpG motifs. *J. Immunol.* 167: 4878–4886.

33. Beloeil, L., M. Tomkowiak, G. Angelov, T. Walzer, P. Dubois, and J. Marvel. 2003. In vivo impact of CpG1826 oligodeoxynucleotide on CD8 T cell primary responses and survival. *J. Immunol.* 171: 2295–3002.

34. Dragoi, A. M., X. Fu, S. Ivanov, P. Zhang, L. Sheng, D. Wu, G. C. Li, and W. M. Chu. 2005. DNA-PKcs, but not TLR9, is required for activation of Akt by CpG-DNA. *EMBO J.* 24: 779–789.

35. Verthelyi, D., and A. R. Zeuner. 2003. Differential signaling by CpG DNA in DCs and B cells: not just TLR9. *Trends Immunol.* 24: 519–522.

36. Krieg, A. M., T. Wu, R. Weeratna, S. M. Efler, L. Love-Homan, L. Yang, A. K. Yi, D. Short, and H. L. Davis. 1998. Sequence motifs in adenoviral DNA block immune activation by stimulatory CpG motifs. *Proc. Natl. Acad. Sci. USA* 95: 12631–12636.

37. Gursel, I., M. Gursel, H. Yamada, K. J. Ishii, F. Takeshita, and D. M. Klinman. 2003. Repetitive elements in mammalian telomeres suppress bacterial DNA-induced immune activation. *J. Immunol.* 171: 1393–1400.

38. Stunz, L. L., P. Lenert, D. Peckham, A. K. Yi, S. Haxhinasto, M. Chang, A. M. Krieg, and R. F. Ashman. 2002. Inhibitory oligonucleotides specifically block effects of stimulatory CpG oligonucleotides in B cells. *Eur. J. Immunol.* 32: 1212–1222.

39. Piccini, M. P. 2005. T cells in pregnancy. *Chem. Immunol. Allergy* 89: 3–9.

40. Renaud, S. J., and C. H. Graham. 2008. The role of macrophages in utero-placental interactions during normal and pathological pregnancy. *Immunol. Invest.* 37: 535–564.

41. Rothenfusser, S., E. Tuma, S. Endres, and G. Hartmann. 2002. Plasmacytoid dendritic cells: the key to CpG. *Hum. Immunol.* 63: 1111–1119.

42. Nardini, E., D. Morelli, P. Aiello, D. Besusso, C. Calcaterra, L. Mariani, M. Palazzo, A. Vecchi, S. Paltrinieri, S. Menard, and A. Balsari. 2005. CpG-oligodeoxynucleotides induce mobilization of hematopoetic progenitor cells into peripheral blood in association with mouse KC (IL-8) production. *J. Cell Physiol.* 204: 889–895.

43. Wood, G. W., E. Hausmann, and R. Choudhuri. 1997. Relative role of CSF-1, MCP-1/JE, and RANTES in macrophage recruitment during successful pregnancy. *Mol. Reprod. Dev.* 46: 62–69.

44. Daley, J. M., A. A. Thomay, M. D. Connolly, J. S. Reichner, and J. E. Albina. 2008. Use of Ly6G-specific monoclonal antibody to deplete neutrophils in mice. *J. Leukocyte Biol.* 83: 64–70.

45. Klinman, D. M. 2006. Adjuvant activity of CpG oligodeoxynucleotides. *Int. Rev. Immunol.* 25: 135–154.

46. Lee, J. G., S. H. Lee, D. W. Park, S. H. Lee, H. S. Yoon, B. R. Chin, J. H. Kim, J. R. Kim, and S. H. Baek. 2008. Toll-like receptor 9-stimulated monocyte chemoattractant protein-1 is mediated via JNK-cytosolic phospholipase A2-ROS signaling. *Cell Signal.* 20: 105–115.

47. József, L., T. Khreiss, D. El Kebir, and J. G. Filep. 2006. Activation of TLR-9 induces IL-8 secretion through peroxynitrite signaling in human neutrophils. *J. Immunol.* 176: 1195–1202.

48. Mor, G., R. Romero, P. B. Aldo, and V. M. Abrahams. 2005. Is the trophoblast an immune regulator? The role of Toll-like receptors during pregnancy. *Crit. Rev. Immunol.* 25: 375–388.

49. Mosca, F., and L. Pugni. 2007. Cytomegalovirus infection: the state of the art. *J. Chemother.* 2: 46–48.

50. Pararas, M. V., C. L. Skevaki, and D. A. Kafetzis. 2006. Preterm birth due to maternal infection: Causative pathogens and modes of prevention. *Eur. J. Clin. Microbiol. Infect. Dis.* 25: 562–569.

51. Hanna, N., L. Bonifacio, B. Weinberger, P. Reddy, S. Murphy, R. Romero, and S. Sharma. 2006. Evidence for interleukin-10-mediated inhibition of cyclo-oxygenase-2 expression and prostaglandin production in preterm human placenta. *Am. J. Reprod. Immunol.* 55: 19–27.

52. Annells, M. F., P. H. Hart, C. G. Mullighan, S. L. Heatley, J. S. Robinson, P. Bardy, and H. M. McDonald. 2004. Interleukins-1, -4, -6, -10, tumor necrosis factor, transforming growth factor-β, FAS, and mannose-binding protein C gene polymorphisms in Australian women: risk of preterm birth. *Am. J. Obstet. Gynecol.* 191: 2056–2067.

53. Kerk, J., D. B. Bartels, M. J. Brinkhaus, C. E. Dammann, T. Dörk, and O. Mammann. 2006. Multiplex measurement of cytokine/receptor gene polymorphisms and interaction between interleukin-10 (-1082) genotype and chorioamnionitis in extreme preterm delivery. *J. Soc. Gynecol. Investig.* 13: 350–356.

54. Menon, R., M. Merialdi, S. J. Lombardi, and S. J. Fortunato. 2006. Differences in the placental membrane cytokine response: a possible explanation for the racial disparity in preterm birth. *Am. J. Reprod. Immunol.* 56: 112–118.

55. Kim, Y. M., M. M. Brinkmann, M. E. Paquet, and H. L. Ploegh. 2008. UNC93B1 delivers nucleotide-sensing Toll-like receptors to endolysosomes. *Nature* 452: 234–238.

56. Latz, E., A. Schoenemeyer, A. Visintin, K. A. Fitzgerald, B. G. Monks, C. F. Knetter, E. Lien, N. J. Nilsen, T. Espevik, and D. T. Golenbock. 2004. TLR9 signals after translocating from the ER to CpG DNA in the lysosome. *Nat. Immunol.* 5: 190–198.

57. Bhan, U., N. W. Lukacs, J. J. Osterholzer, M. W. Newstead, X. Zeng, T. A. Moore, T. R. McMillan, A. M. Krieg, S. Akira, and T. J. Standiford. 2007. TLR9 is required for protective innate immunity in Gram-negative bacterial pneumonia: role of dendritic cells. *J. Immunol.* 179: 3937–3946.

58. Liese, J., U. Schleicher, and C. Bogdan. 2007. TLR9 signaling is essential for the innate NK cell response in murine cutaneous leishmaniasis. *Eur. J. Immunol.* 37: 3424–3434.

59. Buhtoiarov, I. N., P. M. Sondel, J. C. Eickhoff, and A. L. Rakhmilevich. 2007. Macrophages are essential for antitumour effects against weakly immunogenic murine tumours induced by class B CpG-oligodeoxynucleotides. *Immunology* 120: 412–423.

60. Alvarez, M. E., J. I. Fuxman Bass, J. R. Geffner, P. X. Calotti, M. Costas, O. A. Coso, R. Gamberale, M. E. Vermeulen, G. Salamone, D. Martinez, et al. 2006. Neutrophil signaling pathways activated by bacterial DNA stimulation. *J. Immunol.* 177: 4037–4046.